Journal of Materials Processing Technology 214 (2014) 1895–1899

Contents lists available at ScienceDirect

Journal of Materials Processing Technology

journal homepage: www.elsevier.com/locate/jmatprotec

# NiTi with 3D-interconnected microchannels produced by liquid phase sintering and electrochemical dissolution of steel tubes

C. Bewerse[a], L.C. Brinson[a,b], D.C. Dunand[a,*]

[a] Department of Materials Science and Engineering, Northwestern University, Evanston, IL 60208, USA
[b] Department of Mechanical Engineering, Northwestern University, Evanston, IL 60208, USA

ARTICLE INFO

*Article history:*
Received 13 January 2014
Received in revised form 18 March 2014
Accepted 4 April 2014
Available online 13 April 2014

*Keywords:*
Shape memory alloys
Powder metallurgy
Liquid phase sintering

ABSTRACT

A process was developed for fabricating 3D fully interconnected microchannels in superelastic NiTi-Nb for bone implant applications by combining spaceholder powder metallurgy and liquid-phase sintering. Pre-alloyed NiTi powders were blended with 3.1 at.% Nb and cold-pressed around a 3D scaffold of carburized steel tubes acting as space-holders. The tubes were then electrochemically dissolved to form orthogonally interconnected microchannels with 400 μm diameter and ~34% volume fraction. Finally, the powder preform was heated to 1185 °C to form a quasi-binary NiTi-Nb eutectic liquid, which liquid-phase-sintered the NiTi powders without filling the microchannels. The resulting continuously bonded matrix contains an additional 16% porosity, for a total structure porosity of ~50%. NiTi-Nb micro-architectured structures have excellent potential as bone implant scaffolds due to the high versatility in channel size, fraction, and spatial arrangement. Fully interconnected 3D microchannels also increase fluid transport within the scaffold, assisting in nutrient delivery and waste transport to and from cells deep within the scaffold.



## 1. Introduction

Porous NiTi structures can be used for actuators, due to their enhanced heat-transfer capability improving transformation kinetics, and for biomedical implants due to their biocompatibility, strain recovery from the shape memory or superelastic effect, and mechanical properties, which can be tailored to be similar to those of bone (Bansiddhi et al., 2008). Fully interconnected porosity in bone implants allows for fluid transport within the structure and for osseo-integration (Karageorgiou and Kaplan, 2005). Several techniques have been developed to create NiTi porous structures with a varying degree of control for the size, shape, volume fraction, and distribution of equiaxed pores. These techniques have been reviewed by Ryan et al. (2006) for porous metals including surface and bulk porosity, by Bansiddhi et al. (2008) focusing on the biocompatibility of these foams, and by Nasab et al. (2010) for application in total joint replacements.

Recently, powder-metallurgy methods have also been developed to create elongated porosity in NiTi. In self-propagating high-temperature synthesis (SHS), interconnected long wavy pores are created (Li et al., 2000), though the technique also creates undesirable NiTi intermetallics that degrade the mechanical properties (Novák et al., 2013). Blends of NiTi powders and inert spaceholder powders such as NaF (Bansiddhi and Dunand, 2007) or NaCl (Bansiddhi and Dunand, 2008) can be sintered or hot-pressed to form a densified NiTi matrix with interconnected equiaxed pores created by subsequent dissolution of the spaceholder phase. Embedding steel meshes as spaceholders within a NiTi powder preform and densifying by hot-isostatic pressing (HIPing), Neurohr and Dunand (2011a) recently demonstrated dense NiTi with 2D interconnected channels after electrochemical dissolution of the steel, a method also demonstrated in Ti and Ti-6Al-4V (Jorgensen and Dunand, 2010).

Recently, liquid phase sintering was demonstrated as a method for pressureless sintering of NiTi powders in the presence of NaCl (Bansiddhi and Dunand, 2009) or Nb wire (Bansiddhi and Dunand, 2011a) spaceholders. This technique was initially used to bond NiTi foils (Grummon et al., 2007) or create shape memory cellular structures (Michailidis et al., 2009). For the powder bonding method, a small amount of Nb powders is blended with NiTi powders and heated above the quasi-binary NiTi-Nb eutectic temperature of 1150 °C, where the Nb reacts with some of the NiTi to form a liquid eutectic with $Ni_{40}Ti_{40}Nb_{20}$ composition (Piao et al., 1992). This liquid wicks between the remaining NiTi powders and fills the space

* Corresponding author at: Department of Materials Science and Engineering, Northwestern University, 2220 Campus Drive, Cook Hall 2036, Evanston, IL 60208, USA. Tel.: +1 847 491 5370.
*E-mail address:* dunand@northwestern.edu (D.C. Dunand).

http://dx.doi.org/10.1016/j.jmatprotec.2014.04.006
0924-0136/

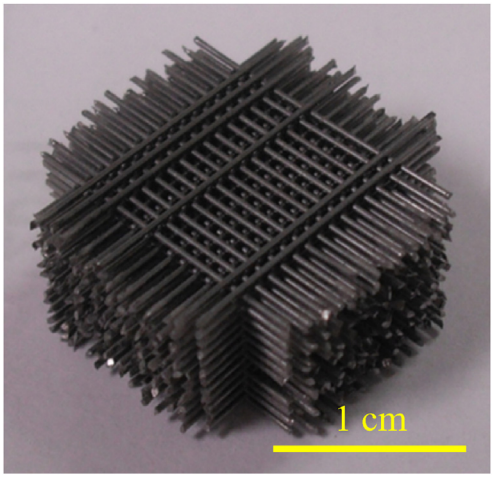


**Fig. 1.** Assembled and sintered spaceholder scaffold constructed with orthogonally stacked 304 stainless steel tubes.

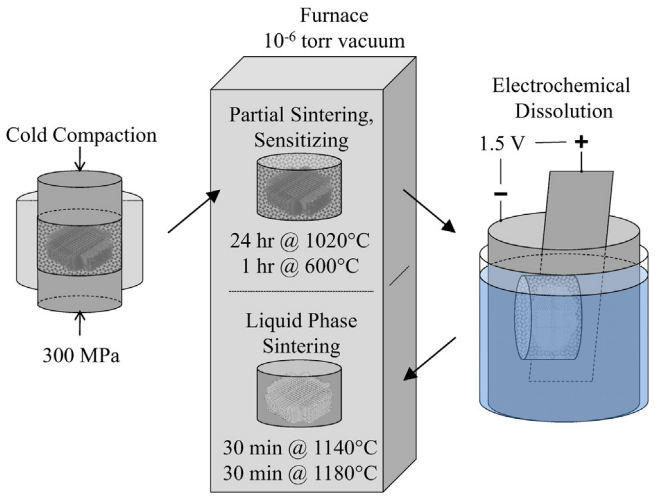


**Fig. 2.** Schematic of the processing steps for fabricating the 3D interconnected microchannel porous structure. The NiTi-Nb powder blend was cold compacted around the steel scaffold and partially sintered. The steel tubes were the sensitized and electrochemically dissolved. After complete removal of the spaceholder, the NiTi-Nb blend was dry sintered, then liquid phase sintered into a densified matrix surrounding the microchannels.

between them, before solidifying into a NiTi-Nb eutectic phase upon cooling in which the NiTi powders are embedded (Bansiddhi and Dunand, 2011b). The solidified NiTi-Nb eutectic is biocompatible (Ng et al., 2010), and foams created by this method, using NaCl as spaceholders, exhibit the shape memory effect with excellent compressive mechanical properties (Bansiddhi and Dunand, 2009).

Here, we develop a technique for creating porous NiTi structures with 3D interconnected organized microchannels by combining the steel spaceholder technique with the Nb-based liquid phase sintering approach. Pre-alloyed NiTi powders were chosen to ensure homogeneous composition and blended with Nb powders to form the liquid phase for pressure-less bonding of the NiTi powders. Commercially available stainless steel tubes were used as the spaceholder to create organized, aligned, and fully interconnected microchannels. Using steel tubes increased the rate of dissolution during removal of the spaceholder, reducing overall production time by a factor of 4 as compared to using steel wires (Neurohr and Dunand, 2011a).

## 2. Experimental methods

Pre-alloyed NiTi powders (Special Metals Corp. Inc.) that have been used in previous research (Neurohr and Dunand, 2011a), with a nominal composition of 51.4 at.% Ti were sieved to 43–63 μm. The NiTi powders were blended with 5.3 wt.% Nb powders (1–5 μm in size, 99.8% in purity, procured from Alfa Aesar) by tumbling for 2 h in a 40 mL glass bottle. According to the liquid eutectic composition of $Ni_{40}Ti_{40}Nb_{20}$, this amount of Nb reacts with 12.3 wt.% NiTi, leading to 16.5 vol.% solidified eutectic and 83.5 vol.% of solid NiTi powders. Tubes made of 304 stainless steel (from Vita Needle, Needham, MA) with an outer diameter of 400 μm and a wall thickness of 150 μm were used as the spaceholder.

The tubes were cut to 19 mm in length, using a high speed abrasive wheel (Dremel) to prevent crimping, and orthogonally stacked into 25 orthogonal layers, with 12 tubes in each layer. Comb-like steel inserts with 500 μm grooves spaced at 500 μm intervals were used to regularly space the tubes with a nominal 1 mm ± 100 μm center to center spacing. The loose tube stack was then sintered within the comb inserts into an interconnected scaffold (Fig. 1) at 1050 °C for 48 h under flowing Ar. The scaffold was then packed in graphite and carburized at 960 °C for 4 h under flowing Ar, cooled and cleaned in acetone to remove all excess graphite.

The NiTi-Nb powder blend was packed around the tube scaffold and cold compacted into a steel die to a pressure of 300 MPa, illustrated in a schematic of the fabrication process in Fig. 2. The resulting NiTi-Nb-steel composite preform was partially sintered under $10^{-6}$ Torr high vacuum at 1020 °C for 24 h, below the eutectic temperature between Ni-Ti-Fe at 1100 °C (Raghavan, 2010), and then cooled and held at 600 °C for 1 h (Parvathavarthini et al., 2012) to sensitize the stainless steel tubes, before cooling to ambient temperature. Sensitizing was performed to decrease the corrosion resistance of stainless steel tubes which were removed from the lightly sintered composite by electrochemical dissolution, as performed in Neurohr and Dunand (2011a) for carbon steel wires. This procedure also prevents interdiffusion between the steel and the NiTi through the formation of a TiC layer at the steel/NiTi interface (Neurohr and Dunand, 2011b). This method was first demonstrated with a steed/Ti-6Al-4V interface, which prevents interdiffusion through the same mechanism (Jorgensen and Dunand, 2011).

The sample was attached with nylon wire to a commercially pure Ti anode, which was centered within a 0.5 mm thickness Ti sheet cathode wrapped around the inside of a 75 mm diameter glass beaker containing an electrolyte of supersaturated NaCl in deionized water. A 1.5 V voltage bias was then applied to dissolve the steel tubes (while NiTi was galvanically protected) under continuous ultra-sonication to remove the dissolution product and refresh the electrolyte at the sample surface. The dissolution procedure was carried out until the current dropped to 0 A, taking 10–12 h on samples with typical 1 mm × 1 mm × 0.5 mm dimensions, and creating a 3D network of microchannels replicating the scaffold of tubes. During dissolution, the electrolyte was refreshed every 2–3 h. At these intervals, the sample was removed from the anode and ultrasonicated in deionized water to remove corrosion products. The sample was then re-attached to the anode, rotated such that a different face was in contact with the anode to achieve more uniform steel dissolution. After full dissolution of the steel tubes, the specimens were dry-sintered at 1140 °C for 30 min under high vacuum ($10^{-6}$ Torr residual pressure), and then subjected to liquid phase sintering for 30 minutes at 1180 °C, above the NiTi-Nb eutectic. The specimens were cooled to room temperature over 2 h in the furnace under $10^{-6}$ Torr high vacuum.

Samples were prepared for optical and SEM microscopy by grinding at 400 and 1200 grit, followed by polishing with 0.05 μm colloidal silica suspension. Scanning Electron microscopy (SEM, Phenom Pro X) was used to examine the microstructure and bonded

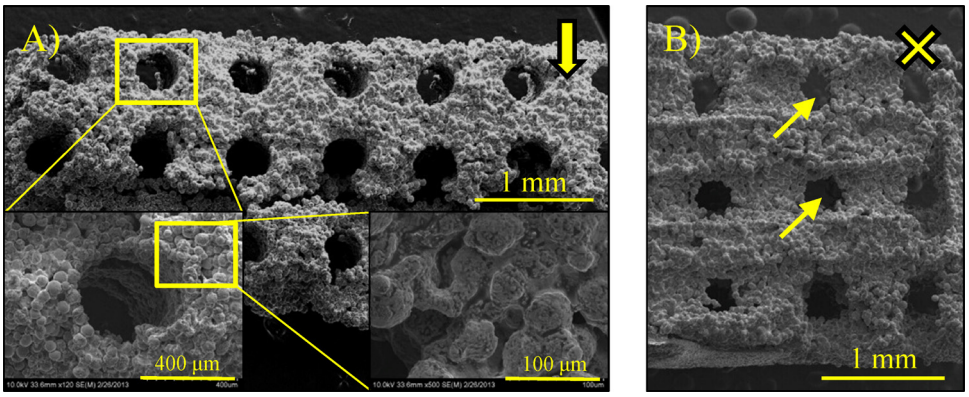


**Fig. 3.** SEM micrographs of the free surface of the as-processed 3D interconnected porous NiTi structure (A) with microchannels fully penetrating the sample (inset) and (B) interconnection windows formed indirectly at intersections of orthogonal tubes. Interconnection windows are indicated with thin arrows, and the thick arrow and X indicate directions parallel and perpendicular to the cold compaction direction, respectively.

powder boundaries, and Energy Dispersive X-Ray Spectroscopy (EDS) was used to determine the composition of phases.

## 3. Results and discussion

### 3.1. Processing considerations

Due to the eutectic reaction in the Ni-Ti-Fe system near 1100 °C (Raghavan, 2010), the steel tube must be fully removed from the specimen before liquid phase sintering is performed above 1150 °C. However the NiTi-Nb powder blend must be bound sufficiently to prevent collapse after removal of the tube spaceholders, so here the structure was partially sintered under high vacuum (1020 °C for 24 h under $10^{-6}$ Torr residual pressure). Ultrasonication, necessary during the dissolution process to remove the dissolved product and refresh the electrolyte, damaged the lightly sintered matrix, preventing mechanical testing of the specimen. The mechanical strength of the lightly sintered NiTi powders could be improved by using smaller diameter NiTi powders or higher cold compaction pressures for better bonding between powders during conventional sintering. Alternatively, a temporary binder such as paraffin wax could be infiltrated through the matrix, and be removed after steel dissolution, just before matrix densification with liquid phase sintering.

### 3.2. Spaceholder considerations

During the sensitization of the stainless steel tube, chromium carbides form at the grain boundaries where they create a chromium-depleted zone which is less corrosion resistant than the bulk of the grains (Parvathavarthini et al., 2012). Preferential corrosion at the grain boundaries thus rapidly dissolves the sensitized tubes by a combination of dissolution and grain crumbling. The tube geometry also allows for penetration of the electrolyte over the whole length of the tube which leads to radial corrosion which is more rapid than the purely longitudinal corrosion of wires used previously (Neurohr and Dunand, 2011b). These two processing innovations combined to decrease the dissolution time by one order of magnitude (i.e., from ~100 h to ~10 h, for a 1 cm × 1 cm × 1 cm of material) as compared to dissolving the same volume of carbon steel meshes in a NiTi matrix (Neurohr and Dunand, 2011b).

Carburization of the stainless steel tubes is also expected to lead to the formation of a TiC layer at the tube surface in contact with the NiTi powders matrix, as previously demonstrated for carburized iron wires within a NiTi matrix (Jorgensen and Dunand, 2010). These authors showed that, without TiC layer, Fe readily diffuses into the NiTi matrix at the sintering temperature of 1020 °C, and that the volume of NiTi matrix containing Fe is subsequently removed by electrochemical dissolution. However, with carburized iron wires, the TiC layer prevented inter-diffusion of Fe into the NiTi matrix, resulting in near direct replication of the dissolved spaceholder into microchannels. As the size of the microchannels is the same as the stainless steel tube spaceholders, we conclude that the same mechanism of TiC formation preventing Fe contamination of the NiTi phase is at work here, and carburization was successful. This enabled use of commercially available stainless steel tubes, commonly used and produced for medical applications. A TiC layer was not visible in the cross-section, and may have been dissolved by the liquid eutectic, or may have spalled during metallographic preparation.

### 3.3. Macrostructure

The fully sintered porous structure is shown in Fig. 3A, with the cold compaction direction indicated by the arrow. Microchannels are well formed after dissolution of the stainless steel tubes and liquid phase sintering of the NiTi matrix. The channels are continuous and regular through the structure, as displayed by the left insert in Fig. 3A. The 400 μm diameter stainless steel tubes were distorted during the uniaxial cold compaction step, resulting in elliptical channel cross sections with a 420 μm major axis perpendicular to the compaction direction and 370 μm minor axis parallel to the compaction direction (corresponding to a 0.88 aspect ratio), as averaged over channel cross-sections on the surface of the sample. The compaction also reduced spacing between the major axis of adjacent channels from 500 to ~460 μm, while minor axis spacing was reduced from 400 μm to ~390 μm as the NiTi-Nb powder blend was packed into the tube spaceholder frame.

The microchannels are also fully connected through fenestrations, creating a porous scaffold with a continuous microchannel network. Previous work with microchannels only has two dimensional interconnectivity (Neurohr and Dunand, 2011a). A view of the structure in Fig. 3B, rotated by 90° as compared to Fig. 3A, clearly illustrates the interconnectivity in the third dimension between layers of the orthogonal microchannels created by the removal of the tubes. Interconnection windows, indicated by thin arrows in Fig. 3B, are not as clearly defined as the channels in the other two dimensions, as they were indirectly formed by the contact point between orthogonal layers of spaceholder tubes. These windows have an average diameter of ~360 μm, and also penetrate the sample, creating a fully interconnected 3D network of channels. This fully continuous network will allow for fluid flow throughout the entire structure with higher permeability than randomly dispersed equiaxed pores connected by narrow windows, as in most existing

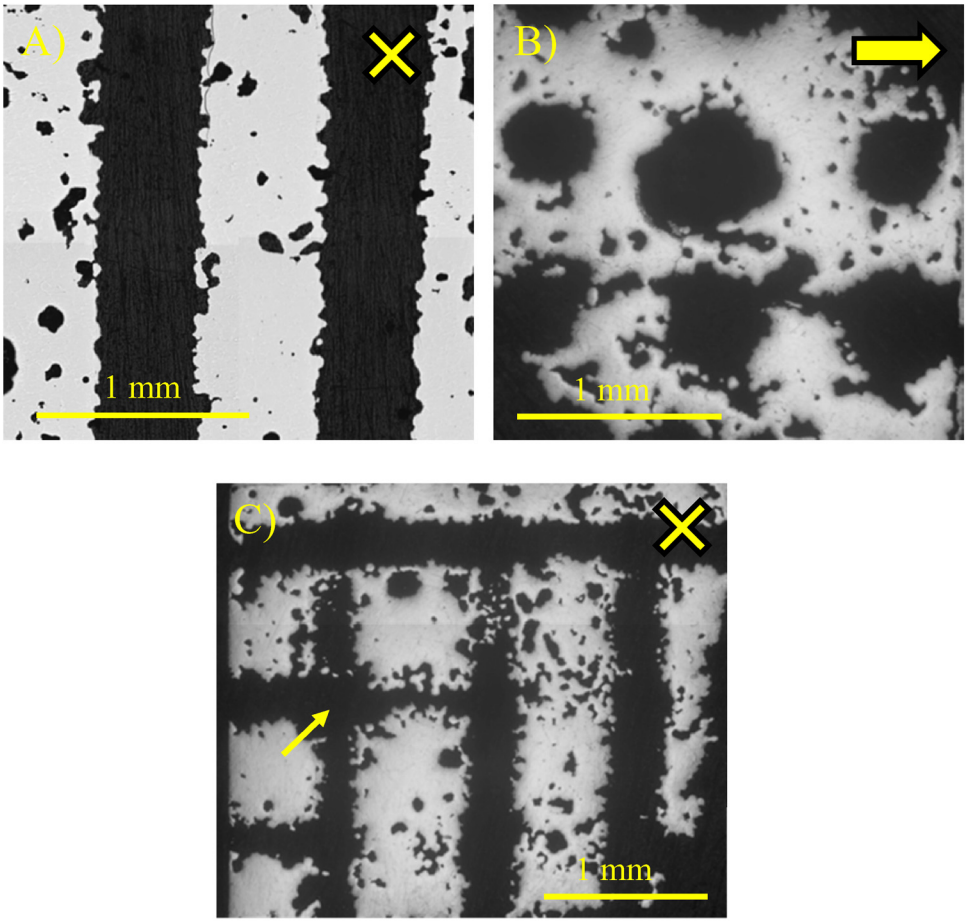


**Fig. 4.** Optical micrographs of 3D interconnected porous NiTi structure cross sections (A) along the length of microchannels, (B) perpendicular to the microchannels, and (C) of the interconnection windows indicated by thin arrows.

NiTi foams. Bone ingrowth is also likely to be much easier within the microchannels, as compared to ingrowth between pores connected by narrow windows found in typical NiTi foams.

### 3.4. Microstructure

Cross-sectional optical micrographs are shown in Fig. 4A–C. The microchannels are easily distinguishable from the NiTi powder matrix, which is continuous but contains microporosity. The microchannels show rough walls, but are mostly uniform in diameter through the length of the sample, as shown Fig. 4A. A second cross section rotated 90° in Fig. 4B illustrates the regular array of channels. The irregular cross section of the channels and their rough texture are again visible. A third cross section in Fig. 4C, similar to that in Fig. 4A but polished at a slight angle from the stacking direction, shows an interconnection window (marked with an arrow) formed at the intersection of two orthogonal channels, as well as top and bottom slices of microchannels slightly above and below the interconnection window. The window is approximately 360 μm in diameter, consistent with SEM observations. The window is not circular like the directly created microchannels, but somewhat rectangular and less defined where the two orthogonal, linear channels intersect.

Fig. 4 shows that NiTi powders are embedded within the NiTi-Nb eutectic. When the eutectic was formed by local reaction of NiTi powders in contact with Nb powders, the liquid wicked into the remaining NiTi powder structure, so that NiTi powders are identifiable on the surface of the walls of the channels. As the liquid wicked away from the channels and into the matrix, it also slightly enlarged the cross section of the microchannels thus reducing the wall thickness between channels. The high wettability of the NiTi powders by the NiTi-Nb liquid eutectic bonds the powders together and prevents the channels from being filled by the liquid.

The matrix surrounding the microchannels contains 15.8 ± 1.1% porosity as measured optically, using polished cross sections of the matrix converted into a binary image where pores were black and matrix was white. The eutectic liquid does not fill additional volume, but rather merges numerous pores between the compacted powders into a smaller number of larger voids in the bonded matrix. Combined with the 34% porosity from the channels, the NiTi structures have an overall porosity of ~50%. Liquid phase sintering, used here for the first time with steel spaceholders, makes the use of specialized hot pressing equipment unnecessary, which has been used in literature to create similar elongated microchannel porous geometries (Neurohr and Dunand, 2011a).

As shown in Fig. 5, the prior surfaces of the NiTi powders are identifiable in SEM micrographs, illustrating that the powders are embedded within a continuous NiTi-Nb eutectic matrix. This microstructure is very similar to those in literature formed by similar liquid phase sintering of NiTi-Nb powder blends (Bansiddhi and Dunand, 2009) with five main phases, identified by grayscale in these backscatter micrographs, where lighter color indicates higher atomic mass. These phases were confirmed here with EDS in Fig. 5. The lightest phase (labeled 1 in Fig. 4) is the eutectic with 20 at.% Nb, filling the space between the NiTi powder (which are the gray regions, labeled 2 with a boundary outlined with a dotted line). Light gray particles, such as the one circled and labeled 3, are small (<1 μm) Nb rich precipitates, which have diffused into the NiTi

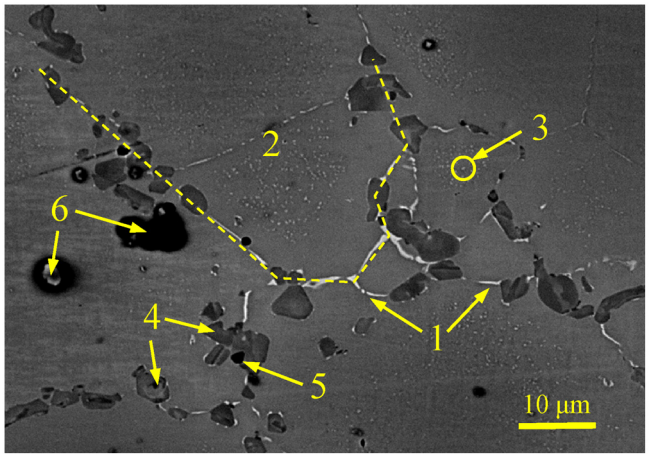


**Fig. 5.** SEM micrograph of NiTi powder boundaries in the liquid phase sintered matrix showing (1) the eutectic region, (2) remaining original NiTi powders, (3) Nb rich precipitates, (4) faceted $NiTi_2$ particles, (5) other Ti rich phases, and (6) voids.

powders then precipitated upon cooling. These are also reported in Siegert et al. (2001). Faceted particles of a darker gray phase (4) are present at the powder boundaries alongside the eutectic phase. These were identified as $NiTi_2$ particles with ~4 at.% Nb, in agreement with phases found in liquid sintered NiTi in literature (Bansiddhi and Dunand, 2009) and also observed in cast $Ni_{45}Ti_{45}Nb_{10}$ (Udovenko et al., 2000). Finally the darkest phase (5) are secondary Ti-rich particles, with Ti content varying from 60 to 90 at.%. Voids and pores are also visible with black contrast, some of which have been identified as (6).

## 4. Conclusions

A novel process to create porous NiTi structures with fully 3D interconnected microchannels using a spaceholder technique and liquid phase sintering was developed. Stainless steel tube spaceholders allow for full control of the geometry, volume fraction, and distribution of the channels within the sample, which can be tailored by varying the tube diameter or stacking configuration. Using tubes also greatly decreases the processing time and ensures full 3D microchannel interconnectivity. The liquid phase sintering used Nb to form a liquid NiTi-Nb eutectic that bonded the solid NiTi powders, creating a continuous matrix with 16% residual porosity that cannot be formed with dry sintering of prealloyed NiTi powders. The resulting NiTi-Nb structures have regular microchannels along two orthogonal directions, connected in the third dimension with windows of the same diameter as the channels. Increased connectivity allows more efficient fluid transport through the structure. The highly regular and fully controllable macrostructure geometry makes these structures interesting candidates for biomedical and actuation applications. In biomedical applications increased fluid transport enables larger scaffold use, with deeper penetration of bone ingrowth. For actuation, fluids with high heat capacity can be circulated through the microchannels to ensure a homogeneous and rapid transformation.

## Acknowledgements

This research was supported by the Office of Army Research, grant number W911NF-12-1-0013/P00002. C.B. also gratefully acknowledges support from the National Defense Science and Engineering Graduate (NDSEG) Fellowship, 32 CFR 168a.

## References

Bansiddhi, A., Dunand, D., 2007. Shape-memory NiTi foams produced by solid-state replication with NaF. Intermetallics 15, 1612–1622.
Bansiddhi, A., Dunand, D.C., 2008. Shape-memory NiTi foams produced by replication of NaCl space-holders. Acta Biomater. 4, 1996–2007.
Bansiddhi, A., Dunand, D.C., 2009. Shape-memory NiTi-Nb foams. J. Mater. Res. 24, 2107–2117.
Bansiddhi, A., Dunand, D.C., 2011a. Niobium wires as space holder and sintering aid for porous NiTi. Adv. Eng. Mater. 13, 301–305.
Bansiddhi, A., Dunand, D.C., 2011b. Processing of NiTi foams by transient liquid phase sintering. J. Mater. Eng. Perform. 20, 511–516.
Bansiddhi, A., Sargeant, T.D., Stupp, S.I., Dunand, D.C., 2008. Porous NiTi for bone implants: a review. Acta Biomater. 4, 773–782.
Grummon, D.S., Low, K.-B., Foltz, J., Shaw, J.A., 2007. A New Method for Brazing Nitinol Based on the Quasibinary TiNi-Nb System. In: 48th AIAA/ASME/ASCE/AHS/ASC Structures, Structural Dynamics, and Materials Conference, April 23–26, Honolulu, Hawaii. American Institute of Aeronautics and Astonautics, pp. 1–7.
Jorgensen, D.J., Dunand, D.C., 2010. Ti-6Al-4V with micro- and macropores produced by powder sintering and electrochemical dissolution of steel wires. Mater. Sci. Eng. A 527, 849–853.
Jorgensen, D.J., Dunand, D.C., 2011. Structure and mechanical properties of Ti-6Al-4V with a replicated network of elongated pores. Acta Mater. 59, 640–650.
Karageorgiou, V., Kaplan, D., 2005. Porosity of 3D biomaterial scaffolds and osteogenesis. Biomaterials 26, 5474–5491.
Li, B., Rong, L., Li, Y., Gjunter, V.E., 2000. A recent development in producing porous Ni-Ti shape memory alloys. Intermetallics 8, 881–884.
Nasab, M.B., Hassan, M.R., Sahari, B., 2010. Bin, metallic biomaterials of knee and hip – a review. Trends Biomater. Artif. Organs 24, 69–82.
Neurohr, A.J., Dunand, D.C., 2011a. Shape-memory NiTi with two-dimensional networks of micro-channels. Acta Biomater. 7, 1862–1872.
Neurohr, A.J., Dunand, D.C., 2011b. Mechanical anisotropy of shape-memory NiTi with two-dimensional networks of micro-channels. Acta Mater. 59, 4616–4630.
Ng, K.W., Man, H.C., Yue, T.M., 2010. Characterization and corrosion study of NiTi laser surface alloyed with Nb or Co. Appl. Surf. Sci. 257, 3269–3274.
Novák, P., Mejzlíková, L., Michalcová, A., Čapek, J., Beran, P., Vojtěch, D., 2013. Effect of SHS conditions on microstructure of NiTi shape memory alloy. Intermetallics 42, 85–91.
Parvathavarthini, N., Kamachi Mudali, U., Nenova, L., Andreev, C., Raj, B., 2012. Sensitization and intergranular corrosion behavior of high nitrogen type 304LN stainless steels for reprocessing and waste management applications. Metall. Mater. Trans. A 43, 2069–2084.
Piao, M., Miyazaki, S., Otsuka, K., Nishida, N., 1992. Effects of Nb addition on the microsctruture of Ti-Ni alloys. Mater. Trans. JIM 33, 337–345.
Raghavan, V., 2010. Fe-Ni-Ti (Iron-Nickel-Titanium). J. Phase Equilibria Diffus. 31, 186–189.
Ryan, G., Pandit, A., Apatsidis, D.P., 2006. Fabrication methods of porous metals for use in orthopaedic applications. Biomaterials 27, 2651–2670.
Siegert, W., Neuking, K., Mertman, M., Eggeler, G., 2001. Influence of Nb content and processing conditions on microstructure and functional properties of NiTiNb shape-memory alloys. Mater. Sci. Forum 394, 361–364.
Udovenko, V.A., Potapov, P.L., Prokoshkin, S.D., Khmelevskaya, I.Y., Abramov, V.Y., Blinov, Y.V., 2000. A Study of the functional properties of alloy Ti-45Ni-10Nb with wide hysteresis of the martensitic transformation. Met. Sci. Heat Treat. 42, 353–356.